Ryerson University
Digital Commons @ Ryerson

1-1-2012

Modeling and Analysis of a Flywheel Energy Storage System for Voltage Regulation

Kamran Masteri Farahani
Ryerson University

Follow this and additional works at: http://digitalcommons.ryerson.ca/dissertations

Part of the Energy Systems Commons

MODELING AND ANALYSIS OF A FLYWHEEL ENERGY

STORAGE SYSTEM FOR VOLTAGE REGULATION

by

Kamran Masteri Farahani, B.A.S.c, Toronto, 2010

A thesis

presented to Ryerson University

in Partial Fulfillment of the Requirements for the

degree of Master of Applied Science

in the program of

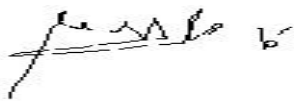Electrical and Computer Engineering

Toronto, Ontario, Canada, 2012

Author's Declaration Page

I hereby declare that I am the sole author of this thesis or dissertation.

I authorize Ryerson University to lend this thesis or dissertation to other institutions or individuals for the purpose of scholarly research.

I further authorize Ryerson University to reproduce this thesis or dissertation by photocopying or by other means, in total or in part, at the request of other institutions or individuals for the purpose of scholarly research.

Thesis Title: modeling and analysis of a flywheel energy storage system for voltage regulation

Degree: Master of Applied Science

Convocation Year: 2012

Student Name: Kamran Masteri Farahani

Graduate Program: Electrical and Computer Engineering

Ryerson University

ABSTRACT

Ontario in 21st century is progressing rapidly to source a bulk of its energy supply from green and renewable energy sources, including wind energy. However there are technical challenges. A significant limiting factor in the large-scale integration of wind energy is the inherent intermittent nature of wind supply.

The purpose of the research project is to develop appropriate control systems to integrate energy storage into the Ontario electricity grid given that energy storage constitutes a fundamental component of a modernized electricity grid. The challenges are multiple. Given that wind generators driven by wind have an output that is intermittent and highly variable, as a result the power supply voltages on distribution lines change at a rapid rate. This research develops a control strategy for the flywheel system to inject or draw real power to or from the connected line on a voltage command, thereby mitigating voltage swings created by variable and intermittent power supply from wind generators.

ACKNOWLEDGEMENTS

DEDICATION

"Dedicated to my beloved family who have provided me encouragement and support throughout my studies"

TABLE OF CONTENT

LIST OF TABLES

LIST OF FIGURES

Chapter 1

INTRODUCTION

1.1   General

Power quality problems such as voltage sags are commonly caused by large wind turbines connected to the far end of long feeders or switching in/out of large loads. Controlling these voltage sags is important aspect in providing a quality supply to customers. In the past, several methods of controlling voltage sags have been investigated such as static var sources, etc. This thesis explores the use flywheel to mitigate power quality problems.

1.2   Introduction to Flywheel

This section provides a gives brief introduction of flywheel, voltage sags, energy storage and topology. In this chapter various systems for protecting industrial processes against voltage sags have been compared (flywheel, static UPS, dynamic voltage restorer, statcom, shunt connected synchronous motor and a transformerless series injector).

A flywheel stores kinetic energy by accelerating a heavy cylindrical mass (flywheel) using an electric motor. To discharge, the flywheel drives a generator to produce electricity. The earliest form of a flywheel is found in the Neolithic spindle and the potter's wheel [1]. The wheel is a disc made of wood, stone or clay. It rests on a fixed pivot and can be rotated around its center. The energy stored in a potter's flywheel

is about 500J, which is by no means negligible [2]. The main disadvantages are friction and material integrity. Most of energy is lost in overcoming frictional losses.

There were two important developments during Industrial Revolution in the nineteenth century: one is the use of flywheels in steam engines and the other is extensive use of iron. Making the flywheels out of iron had the benefit of greater material integrity. Also they could be built in a single piece and could handle more mass and moment of inertia compare to other flywheels in the same volume.

More recently, the ability of a flywheel to deliver high power in a short time has been used in applications such as mechanical presses, lubrication or cooling pumps, mine locomotives, inertial friction welding and inertial starters.

By development of science towards the use of high-strength composite materials, the new generation flywheels were made. These new flywheels can store more energy at higher speeds for a given mass than a steel flywheel. It was after this breakthrough that engineers thought of using a composite flywheel energy storage system for electric vehicles and stationary power backup [20].

Flywheels store energy in the form of kinetic energy. The amount of energy 'E' stored in a flywheel varies linearly with moment of inertia 'I' and with the square of the angular velocity 'ω'.

$$E = \frac{1}{2} . \text{I.} \, \omega^2 \tag{1.1}$$

The moment of inertia is a physical quantity, which depends on the mass and shape of the flywheel. It is defined as the integral of the square of the distance 'x' from the axis of rotation to the differential mass 'dm_x'.

$$\text{I} = \int X^2 \, dm_x \tag{1.2}$$

2

The solution for a cylindrical flywheel of mass 'm' and radius 'r' will be:

$$I = m.r^2 \qquad (1.2a)$$

and

$$E = \frac{1}{2}.m.r^2.\omega^2 \qquad (1.2b)$$

Since the energy stored is proportional to the square of angular velocity, increasing the angular speed increases stored energy more effectively than increasing mass. On the other hand, increasing angular speeds result in increased frictional losses and hence thermal problems. With the help of magnetic bearing technology, the frictional losses due to bearings can be overcome, but at the expense of reliability. Also the energy stored can be expressed in terms of peripheral velocity 'v', which is defined as the product of perpendicular distance from the axis of rotation and angular speed as:

$$v = r.\omega \qquad \text{or} \qquad E = \frac{1}{2}.m.v^2 \qquad (1.3)$$

The tensile strength, 'σ', of the material limits the peripheral velocity, and hence the amount of energy stored. For a mass density 'ρ', the tensile strength is defined as:

$$\sigma = \rho.v^2 \qquad (1.4)$$

Energy density is a term generally used to characterize an energy storage system. Usually high energy density is preferred, but this can pose thermal problems. Energy density, 'E_m', is loosely defined for a flywheel as the ratio of energy stored to its mass:

$$E_m = \frac{1}{2}.r^2.\omega^2 \qquad (1.5)$$

The volume energy density, 'E_V', is obtained by substituting 'm' in the stored energy equation, as the product of volume and the mass density:

$$E_V = \frac{1}{2}.\rho.r^2.\omega^2 \qquad (1.6)$$

Therefore, if the dimensions are fixed, the maximum energy stored per volume 'E_{vmax}' depends on the tensile strength of the material as:

$$E_{Vmax} = \frac{1}{2}.\sigma_{max} \qquad (1.7)$$

where 'σ_{max}' is the maximum tensile strength of the flywheel material.

Similarly the maximum energy stored per mass 'E_{mmax}' is

$$E_{mmax} = \frac{1}{2}.\frac{\sigma_{max}}{\rho} \qquad (1.8)$$

Therefore, the maximum energy storage capacity can be achieved by using a material with a low density and high tensile strength. Depending on the application, either volume energy density or mass energy density takes precedence during the design stage. For a transportation application, mass energy density is a major consideration, since mass is a limiting factor.

The energy density expressions above apply for a simple rim type flywheel. There are many designs for flywheels, and the general expression of maximum energy stored per mass is:

$$E_{mmax} = K.\frac{\sigma_{max}}{\rho} \qquad (1.9)$$

where 'K' is defined as the flywheel shape factor, which depends on the geometry of the flywheel. The flywheel shape factors for several different types of flywheels are given in Table 1.1.

The value of 'K' is obtained from the equation for the moment of inertia (1.2). The stress distribution in a flywheel due to centrifugal loading becomes complex for shape factors greater than 0.5, and a detailed analysis needs to be done to safely achieve it.

For low speed flywheels, the best way to maximize stored energy is by increasing moment of inertia. A massive rim or disc made of high density material such as cast iron or steel is sufficient in these cases. The main advantages of low speed flywheels are that they use a well-established technology and they are cheaper to build. [2]

For high-speed applications, small discs with a constant stress profile, built with a low density and high strength materials, are better for maximizing energy density. The most commonly used composite material is Kevlar, a plastic material reinforced with glass, carbon or aramid fibers. The main disadvantage of this material is its high cost. The cheapest composite material is S-glass, but this material has lower fatigue strength. The specific strengths of different flywheel materials are listed in Table 1.2. A comparison of flywheel energy storage capabilities is given in Table 1.3. [2]

There is also a safety factor, which limits the amount of stored energy available for discharge [3]. When this is considered, the useful energy stored per mass is given by:

$$E_m = (1 - S^2).K.\frac{\sigma}{\rho} \tag{1.10}$$

where 'S' is the ratio of minimum to maximum operating speed, usually set at 0.2. So the maximum amount of energy stored doesn't depend directly on inertia or on the

5

angular velocity, since either of these can be chosen independently to obtain the required design stress. And within the design stress, the amount of energy stored is linearly proportional to the moment of inertia and to the square of its angular velocity.

Flywheel Shape	K
Constant stress disk	0.931
Constant thickness disc	0.606
Thin rim	0.500
Constant stress bar	0.500
Rod or circular brush	0.333
Flat pierced disc	0.305

Table 0.1 Flywheel Shape Factors [2]

Flywheel Material	Specific Strength(kJ/kg)
Cast iron	19
Carbon steel	44
Alloy steel	100
Wood	130
Kelvar	1700
S-glass	1900
Graphite	8900

Table 0.2 Specific strengths of flywheel materials [2]

Material	Density $(10^3 \frac{kg}{m^3})$	Useful Energy$(10^3 \frac{J}{kg})$	Mass of the Flywheel$(10^3 kg)$
Wood birch	0.55	21.0	1720
Mild steel	7.80	29.5	1220
S-Glass	1.90	70.5	509
Maraging steel	8.00	86.4	417
Carbon 60% fibre	1.55	185.4	194
Kevlar 60% fibre	1.40	274.3	131

0.3 Comparison of typical flywheel energy storage capabilities [3]

New designs of flywheel include the improvement of driving program for generating motor. It is done to increase the rotational speed of a compact flywheel energy storage system that uses a superconducting magnetic bearing (SMB) and a permanent magnet bearing (PMB)[14].

1.3 Literature Survey: Electrical Energy Storage and Topologies

This section discusses different available electrical energy storage technologies and the reason for preferably using flywheel energy storage.

Energy can neither be created nor destroyed. But it can be transformed from one form to another. Electrical energy is the form of energy that can be transmitted efficiently and easily transformed to other forms of energy. The main disadvantages with electrical energy involve storing it economically and efficiently. Electrical energy can be converted and stored in different forms:

- Electrochemical Energy
- Electrostatic Energy

- Electromagnetic Energy

- Electromechanical Energy

1.3.1 Electrochemical Energy Storage

In this type of storage, electrical energy is converted and stored in the form of chemical energy. There are two main categories: batteries and fuel cells [3]. Batteries use internal chemical components for energy conversion and storage whereas fuel cells use synthetic fuel (for example Hydrogen, methanol or hydrazine) supplied and stored externally. Both use two electrodes, an anode and a cathode, that exchange ions through an electrolyte internally and exchange electrons through an electric circuit externally. The Lead-acid battery, discovered by Plante in 1859, is the most widely used battery. The battery consists of pairs of lead electrode plates immersed in a dilute sulphuric acid that acts as an electrolyte. Every alternate lead plate is coated with lead dioxide. Discharging results in the conversion of both of the electrodes to lead sulphate. Charging restores the plates to lead and lead dioxide. The physical changes in electrodes during charging and discharging deteriorates the electrodes and hence reducing their life. The main advantages are they have a well-established technology. The main drawbacks with batteries are:

- Slow response during energy release

- Limited number of charge discharge cycles

- Relatively short life time

- High internal resistance

- Low energy density

- Maintenance requirements for some types

- Environmental hazards

8

W. R. Grove demonstrated the first hydrogen-oxygen fuel cell in 1839. The by-product of a Hydrogen fuel cell is water. By electrochemical decomposition of water into hydrogen and oxygen and holding them apart, hydrogen fuel cells store electrical energy. During discharge, the hydrogen is combined with oxygen, converting the chemical energy to electrical energy. The main advantages are environment friendly. The main drawbacks with fuel cells as energy storage elements are:

- Slow response during energy release

- Temperature dependence

- Corrosion problems

- Hydrogen storage

- Inefficient transfer of electrical energy to chemical energy

1.3.2 Electrostatic Energy Storage

Electric energy can be converted and stored in the form of electrostatic field between the parallel plates of a charged capacitor. The amount of energy stored is proportional to square of the voltage across the parallel plates and to its capacitance. For a fixed voltage, the volume energy density for a parallel plate capacitor is proportional to capacitance, which is proportional to the permittivity of the insulator between the parallel plates. Most of the insulators have relative permittivity in the range of 1 to 10. Due to the small capacitance, ordinary capacitors can store very limited amount of energy. Ultra-capacitors use electrochemical material for improving permittivity and hence energy density. They require less maintenance and have much longer lifetimes compared to batteries. They have high energy density and do not have moving parts. The main drawbacks with capacitors are:

- Cost

- Temperature dependence

- Not rugged

1.3.3 Electromagnetic Energy Storage

Electric energy can be converted and stored in the form of an electromagnetic field. A Superconducting magnetic energy storage (SMES) coil consists of a superconducting coil carrying large DC currents. The amount of energy stored is proportional to the square of the DC current flowing through the coil and to its inductance. The volume energy density is proportional to the permeability of the material used for the coil. In order to keep the temperature of the superconductor below its critical temperature, a cryogenic cooling system is required. Increasing the DC current increases the amount of energy stored. Once the current in the coil reaches its maximum value, the voltage across it is zero and the SMES is fully charged. This storage scheme has very low losses due to negligible resistance in the coil. Also SMES coils can be built for larger energy and power. The main drawbacks with SMES are:

- Cost

- Reliability in maintaining cryogenic cooling

- Compensation of external stray fields

- Electromagnetic forces on the conductors

- Bulk/volume

1.3.4   Electromechanical Energy Storage

Electrical energy can be converted and stored in the form of kinetic energy in a flywheel. Motor/generator sets, DC machines and induction machines are used for energy conversion. The amount of energy stored in a flywheel is proportional to the square of angular velocity and to its inertia for a given design stress.

The energy storage technologies discussed above have their own advantages and disadvantages but the following advantages make flywheels a viable alternative to other energy storage systems:

- Low cost

- High power density

- Ruggedness

- Greater number of charge discharge cycles

- Longer life

- Less maintenance

- Environmental friendly

- Fast response during energy release

Flywheels can be designed for low speed or high-speed operation. A low speed flywheel has advantages of lower cost and the use of proven technologies when compared to a high-speed flywheel system. The main disadvantages are:

- less energy stored per volume

- higher losses

- increased volume and mass

1.4   Power Quality

Sags are known to be among the most costly power quality phenomena in industry. Different solutions exist to reduce the costs incurred due to sags: they are often structured in the four categories listed in Figure 1.1 [5].

1. Equipment specification
2. Protective control
3. Overall protection inside the plant
4. Utility solutions
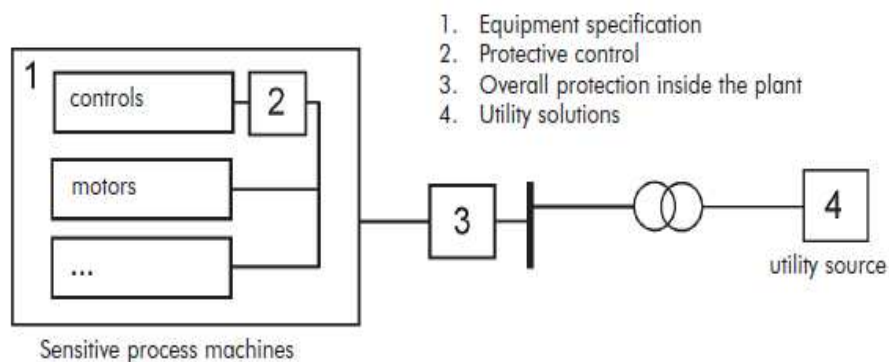
Figure 1.1 Possible sag mitigation method

Modifications in the process equipment itself (Number 1 and 2 in Figure 1.1) tend to be the cheapest to implement but are not always possible because manufacturers have not made suitable equipment readily available in the market. Modifying the grid, (Number 4 in Figure 1.1), although an interesting option, is not always possible and is likely to be very expensive. The only methods that can generally be applied are protective measures installed between the sensitive process and the grid (Number 3 in Figure 1.1), and these are discussed in this section.

In theory, installing an uninterruptible power supply (UPS) is the easiest way to protect sensitive processes against all sags. However, due to its considerable purchase and maintenance costs, UPS equipment is installed on a structural basis only in places where the damage resulting from power supply problems is very high, such as in hospitals, computer facilities and financial institutions. In other cases, including most

industrial processes, the installation of protective equipment must be subject to a cost-benefit analysis, which often shows that installing a UPS is too expensive [6].

This section discusses some of the physical and performance characteristics of various voltage-sag protective product categories currently available on the market in comparative terms. For each type, each characteristic is indicated as an advantage (+), neutral (=) or as a disadvantage (-).

Size

Some systems are currently only available in sizes larger than 1 MW (-), while others are also sold in sizes smaller than or equal to 100 kW (+).

Purchase cost

Since the decision to buy mitigation equipment to prevent damage due to voltage sags is the outcome of a cost-benefit analysis, the purchase price of the system is very important. Although contracts are made on an individual basis and can vary substantially, rough guidelines are provided for the purchase and installation cost of a medium-sized (between 100 kVA and 500 kVA) device if available. Three price categories are defined:

- : > 250 euro per kVA

= : 150-250 euro per kVA

+ : < 150 euro per kVA

Maintenance

Depending on the type of system, the maintenance costs may be substantial. This section only distinguishes whether annual maintenance is required (-) or not (+).

Efficiency

Many systems require continuous electricity demand due to the use of power electronics, the use of moving parts (flywheel) or cooling (SMES), resulting in a reduction of the overall efficiency. Three categories are distinguished:

+ : losses <0.5% of rated power

= : losses 0.5-2% of rated power

- : losses >2% of rated power

Reaction time

Some of the protection devices need to detect the voltage sag before they can react. This may result in transient process behaviour. The reaction (activation) time of the protective device is divided into three categories:

+ : reaction or activation transient < 1 ms

= : transient 1-5 ms

- : transient > 5 ms

Voltage harmonics

Some of the mitigation systems are also able to continuously compensate for voltage harmonics originating from the supplying network (+) while others do not influence voltage harmonics (=).

Current harmonics

If the downstream load contains many power electronic applications, such as variable speed drives, the current will be highly non-linear. Some voltage sag mitigation systems have the ability to draw a linear current from the network despite the non-linear loads (+), while others do not influence current harmonics (=).

<u>Reactive power</u>

Some applications have the ability to supply or draw reactive power continuously (+) while others cannot (=).

<u>Summary</u>

Table 1.4 summarises the performance of the described systems with regard to these parameters.

	Size	Purchase cost	Maintenance	Efficiency	Reaction time	Voltage harmonics	Current harmonics	Reactive power
Flywheel	+	-	-	-	=	+	+	+
Static UPS	+	-	-	-	+	+	+	+
DVR-1	+	+	+	=	=	=	=	+
DVR-2, 200% load	-	-	+	-	=	+	=	=
DVR-2, 400% load	-	=	+	-	=	+	=	=
Statcom-SMES	-	=	-	=	-	=	=	+
Shunt connected SM	+	=	-	-/=	=	+	+	+
Transformerless series injection	+	=	+	+	=	=	=	=

Table 1.4 Technical and economic aspects of different mitigation methods

If we consider the characteristics of the new flywheel system designed by Temporal Power, then the negative point for efficiency of the flywheel could be overcome and thus change to positive as well, which makes it a superior option.

1.5 Voltage Sags

Voltage sag as defined by IEEE Standard 1159-1995, IEEE Recommended Practice for Monitoring Electric Power Quality, is a decrease in RMS voltage at the power frequency for durations from 0.5 cycles to 1 minute, reported as the remaining voltage.

Voltage sags can occur on utility systems both at distribution voltages and transmission voltages. Voltage sags that occur at higher voltages will normally spread through a utility system and will be transmitted to lower voltage systems via transformers.

One of the most worrying trends is the integration of wind energy in distribution and transmission networks which are exposed to voltage sags. The behaviour of the wind turbine is important not only under normal working conditions but also when voltage sags do occur. In some countries, especially those where there are large wind energy installations, Transmission System Operators (TSO) and Distribution System Operators (DSO) are particularly concerned about this problem, consequently their Grid Codes are continuously being revised. Voltage sags are becoming an increasing concern due to the sensitivity shown by the wind generation, caused by the adjustment of protective devices, especially in wind turbines that use power electronics to support a Double-Fed Induction Generator (DFIG). As a result, many grid codes establish immunity levels against voltage sag.

In Ontario under pre-contingency conditions with all *facilities* in service, or with a critical element(s) out of service after permissible control actions and with loads modeled as constant MVA, the *IESO controlled grid* is to be capable of achieving acceptable system voltages. The table below indicates the maximum and minimum voltages generally applicable. These values are obtained from Chapter 4 of the "Market Rules"*,* and CSA standards for distribution voltages below 50 kV [4].

				Transformer Stations, e.g. 44, 27.6, 13.8 kV
Nominal Bus Voltage (KV)	500	230	115	
Maximum Continuous (KV)	550	250	127*	106%
Minimum Continuous (KV)	490	220	113	98%

Table 01.5: Pre-Contingency Voltage Limits

* However certain buses can be assigned specific maximum and minimum voltages as required for operations. In case of Wind Turbine generators these limitations are stiffer and voltage is bounded within 1% of its nominal value.

1.6   Objective of this Thesis

This thesis aims to develop an optimal control strategy for flywheel systems to regulate feeder voltages. The control model considers both the flywheel system and the connected distribution system feeder characteristics to determine the optimal settings for the flywheel such that feeder voltages are held nearly constant.

For simulation, an induction machine is used for bi-directional transfer of energy to the flywheel. Two voltage sourced converters share a common DC link constitute the power electronic interface between the electricity grid and the induction machine. This power electronic interface is used for the bi-directional flow of energy for charging and discharging the flywheel – a mechanical battery – through the induction machine with DC link as medium. An inner control system is used to generate gate pulses for each converter. Using an optimization algorithm, an outer control system detects voltage sag and regulates the voltage at the point of common coupling with the electricity grid.

This thesis presents the modeling, simulation and analysis of a flywheel energy storage system (FESS) for voltage regulation.

1.7   Chapter-wise Outline

The system configuration and control system modeling was done using MATLAB/Simulink and is explained in Chapter 2. The proposed voltage regulation is presented in Chapter 3. The simulated performance of the flywheel energy storage system in mitigating voltage sag is analyzed in Chapter 4.

Chapter 2

System Configuration and Control System

2.1   System Configuration

The basic circuit consists of an energy storage system, power electronic interface LCL filter and a three phase source that represents electric grid system as shown in Fig. 2.1. The energy storage system in this case is a flywheel coupled to an induction machine. The induction machine is used for energy conversion. The power electronic interface consists of two voltage sourced converters connected through a common DC link [18]. One voltage source converter interfaces with the energy conversion and storage system and the other with the electric grid system.

The flywheel energy storage system has three modes of operation:

- Charge mode

- Stand-by mode

- Discharge mode

During charge mode, the VSC interfacing the electric grid system runs as a rectifier and the other as an inverter, with the transferred energy accelerating the flywheel to its rated speed. In this mode, energy is stored in the flywheel in the form of kinetic energy. The energy flow is from grid system to flywheel with induction machine as energy converter.

Once the flywheel reaches its charge speed, the storage system is in standby mode and is ready to discharge when the PCC bus sees a voltage sag.

During discharge mode, the VSC interfacing the grid system runs as an inverter injecting the required voltage in series with the line to correct the voltage sag. The flywheel VSC runs as a rectifier. The flywheel slows as it discharges. In this mode, the stored energy is used for sag correction and energy flow is from the flywheel to hydro grid system [15].
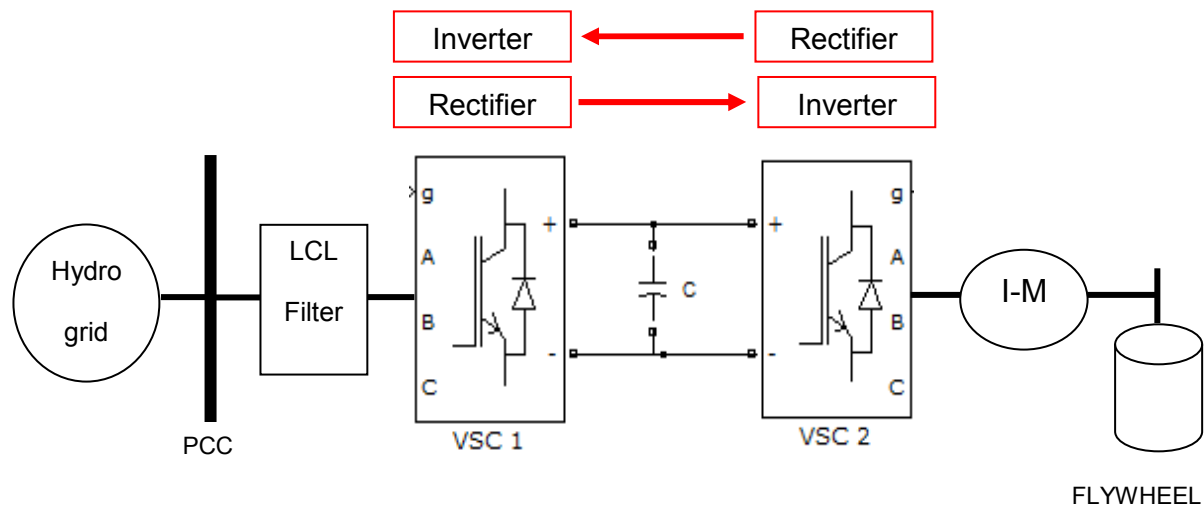
Figure 2.1 Basic circuit of flywheel energy storage system

2.2   Controlling Strategy

A Flywheel energy storage system consisting of the following components that were modeled in MATLAB/Simulink:

- Two voltage sourced converters

- Induction machine

- Flywheel

- Control system

Fig. 2.2 shows a single line diagram of a flywheel energy storage system. To simplify modeling and testing, it is broken into two sub models. Each sub model is separately modeled, tested and integrated to make it a complete model. The sub models are:

• Field oriented control model

• Voltage oriented control model
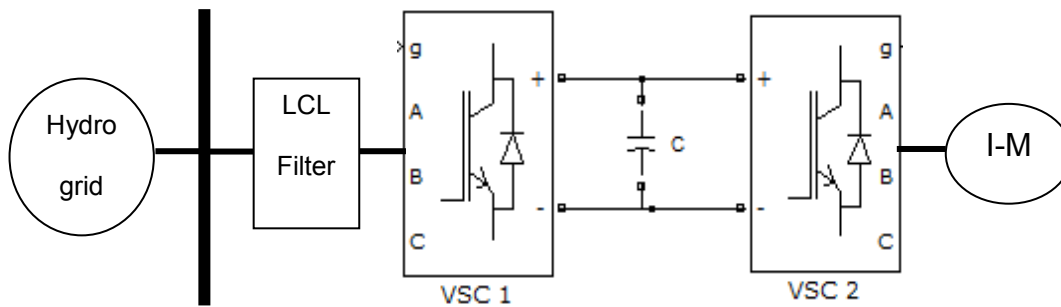
Figure 2.2 Single Line Diagram of a flywheel energy storage system

2.2.1 Field Oriented Control

Fig. 2.3 shows the outline of the field oriented control drive that was modeled in SIMULINK. It has the following sub models [16]:

- Induction machine model

- Field oriented controller model

- DC link capacitor for DC voltage regulation

- Voltage sourced converter
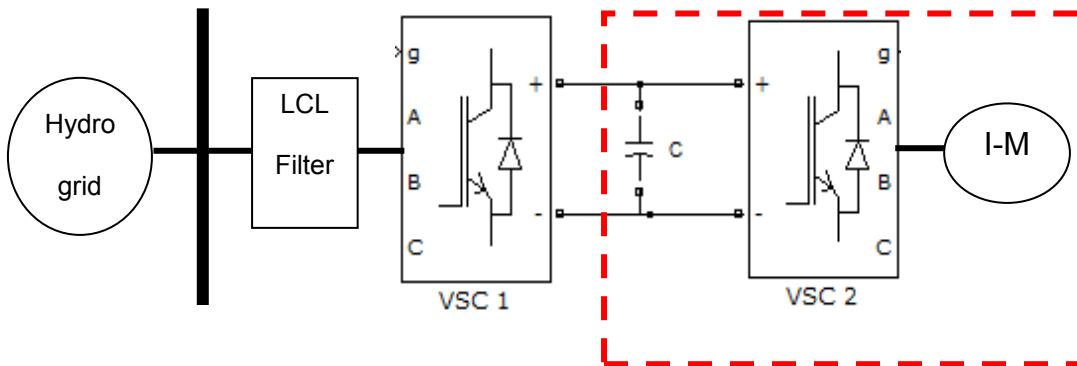
Figure 2.3 Field Oriented Control Model Breakup

The performance of this model was found adequate for the purposes of controlling voltage at the point of interconnection. The control meets and exceeds requirements as set by Canadian Standard Association guidelines.

2.2.2 Voltage Oriented Control

Fig. 2.4 shows the outline of a voltage oriented control as it was modeled in Simulink. It has the following sub models [17]:

- 3-phase AC power supply
- Series transformer and filters
- Voltage sourced converter
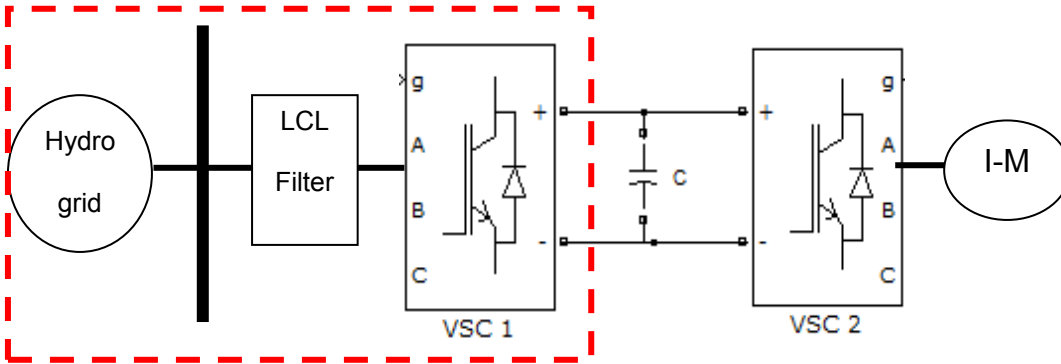
Figure 2.4 Voltage Oriented Control Model Breakup

This model was modeled on Matlab/Simulink environment. Simulation tests show that the system adequate and meets requirements when the system parameters are appropriately designed. Tests were conducted on site to verify if the response times and control is adequate. The lab tests also confirm this aspect.

2.3   Summary

In this chapter available control strategies are modeled and tested. The voltage oriented control is chosen for further work as a physical model is readily available.

Chapter 3

PROPOSED VOLTAGE REGULATION

3.1 Introduction

This chapter focuses on the design of an algorithm to regulate the voltage at PCC using Temporal Power flywheel. The optimization algorithm reveals the necessary amount of 'P' and 'Q' that the flywheel has to generate in order to keep the PCC voltage within the limit (1% Error). To optimize the 'P' and 'Q' generated by the flywheel, the minimum value of Apparent Power 'S' has to be found using MATLAB.

Also to see the effect of having Active power involved in voltage regulating, the case of injecting only Reactive Power ($P_{flywheel} = 0$) from the flywheel has been considered and its result has been compared to the case that $P_{flywheel} \neq 0$. Finally, the size of the flywheel is obtained, considering the maximum amount of P and Q needs to be generated to regulate the voltage at PCC.

3.2 Tasks to Solve the Problem

1- Use a sample distribution system with a wind generator akin to Hydro One's system.

2- Transform the 96 bus system to the 2 bus system, considering the system is unbalanced.

  a) Perform a power flow analysis on Hydro-One data (96 bus System) in order to find bus voltages (using PSS®E 32).

  b) Change the loads from constant-power-loads to constant-admittance-loads.

24

c) Determine the Thevenin voltage of the 96 bus system (using PSS®E 32).

d) Write a program that creates the Y bus matrix of the 96 bus system. (Considering Constant-Admittance-Loads, Shunts, Charging and Tap Ratios in Y bus matrix using MATLAB)

e) Determine the Thevenin impedance of the 96 bus system using theories related to the Y bus matrix.

f) Test the 2 bus Thevenin system characteristics and see if it matches the 96 bus system using PSS®E 32.

3- Based on the 2 bus system, design an optimization algorithm which calculates the necessary amount of $P_{flywheel}$ and $Q_{flywheel}$ in order to keep V_{PCC} within the limit.(Using MATLAB)

4- Program the control drives so it recognizes the optimized $P_{flywheel}$ and $Q_{flywheel}$ values as its reference, (using SYPY Pro):

a) Create Look-Up tables according to the algorithm result.

b) Write a program that uses the Look-Up table and linear interpolation technique.

5- Perform a test at Temporal Power location.

3.3 Thevenin Theorem

Thevenin's theorem states that it is possible to reduce any linear circuit to an equivalent circuit with just a single voltage source and series impedance. It is especially useful in analyzing power systems and other circuits where one particular resistor in the circuit (called the "load" resistor) is subject to change, and re-calculation of the circuit is

necessary with each trial value of load resistance, to determine voltage across it and current through it.

<u>Steps to follow for Thevenin's Theorem:</u>

1) Find the Thevenin source voltage by removing the load resistor from the original circuit and calculating voltage across the open connection points where the load resistor used to be.

2) Find the Thevenin resistance by removing all power sources in the original circuit (voltage sources shorted and current sources open) and calculating total resistance between the open connection points.

3) Draw the Thevenin equivalent circuit, with the Thevenin voltage source in series with the Thevenin resistance. The load resistor re-attaches between the two open points of the equivalent circuit.

4) Analyze voltage and current for the load resistor following the rules for series circuits.

3.4   Thevenin Voltage Of The 96-Bus System

In this case, positive sequence is being tested, considering the system is unbalanced.

According to the theory the wind-turbine generator has been disconnected in order to find the open circuit voltage at Bus-7081(Wind-turbine bus).
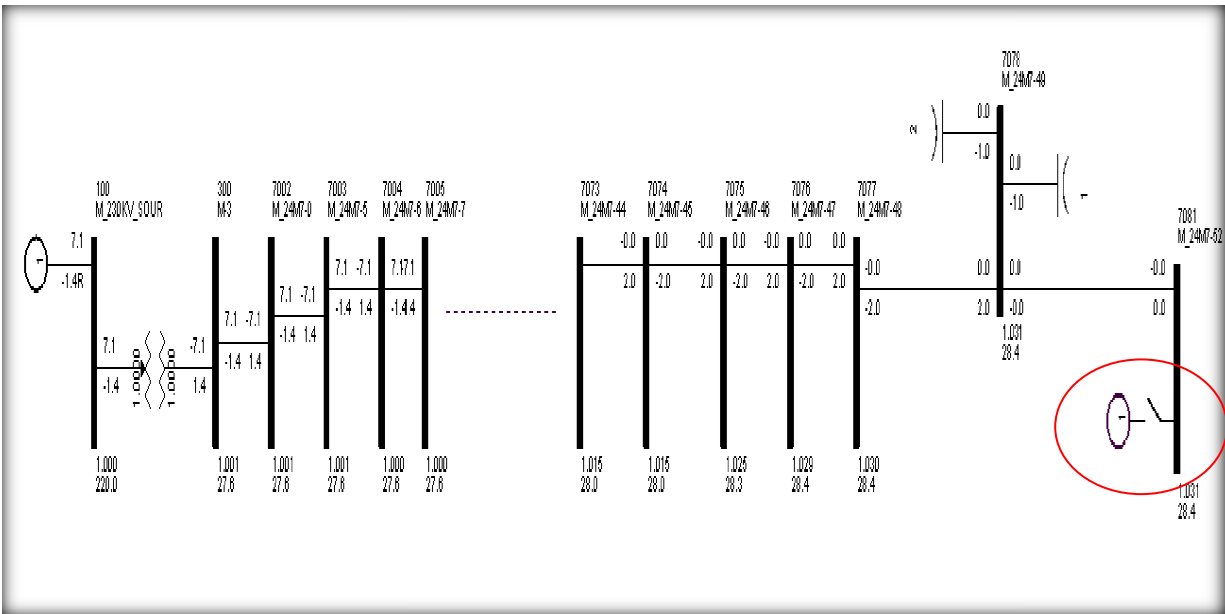
Figure 3.1: wind-turbine generator bus is open in H.O.N.I. 96 bus system

By doing load flow analysis using PSSE, it can be seen from Figure 3.1 that:

per-unit

3.5   Thevenin Impedance Of The 96-Bus System

For this experiment 100% load capacity and positive sequence voltages are being used. In order to find the Thevenin impedance, the first step is to change the loads to constant-admittance loads and then the Y-Bus matrix has to be created and the last step is to use the relationship between thevenin's theorem and bus impedance matrix.

Steps to calculate the Constant-Admittance-Loads:

1)   and   of the loads are known, therefore we perform a power flow analysis on Hydro-One data (96 bus System) in order to find bus voltages V (using PSSE).

2) The following formula is known

$$S_{Load} = P_{Load} + jQ_{Load} \tag{3.1}$$

3) We also know that:

$$S_{Load} = \frac{V^2}{Z_L} = V^2 \times Y_{C.A.L} \tag{3.2}$$

4) From (3.1) and (3.2) =>

$$V^2 \times Y_{C.A.L} = P_{Load} + jQ_{Load} \tag{3.3}$$

$$Y_{Constant-Admittance-Load} = \frac{P_{Load} + jQ_{Load}}{V^2} \tag{3.4}$$

and

$$Y_{C.A.L} = G_{C.A.L} + jB_{C.A.L} \tag{3.5}$$

Therefore:

$$G_{C.A.L} = \frac{P_{Load}}{V^2} \tag{3.6}$$

$$B_{C.A.L} = \frac{Q_{Load}}{V^2} \tag{3.7}$$

Y-Bus Matrix:

The second step to find the Thevenin impedance is to create the Y-bus matrix. It had to be created in a way that includes all the elements of the 96 bus system (using MATLAB).

In power engineering, Y-bus is an n x n symmetric matrix describing a power system with n buses. It represents the nodal admittance of the buses in a power system.

$$Y = \begin{bmatrix} Y_{11} & Y_{12} & \cdots & Y_{1n} \\ Y_{21} & Y_{22} & \cdots & Y_{2n} \\ \cdots & \cdots & \cdots & \cdots \\ Y_{n1} & Y_{n2} & \cdots & Y_{nn} \end{bmatrix} \tag{3.8}$$

The admittances Y_{11}, Y_{22}, ... Y_{nn} are called the self-admittances at the nodes, and each equals to the sum of all the admittances terminating on the node which includes:

Tap ratios, Line Charging, Constant-Admittance-Loads and Shunt Capacitors

$$Y_{nn} = \frac{Y_n}{a_n^2} + B_n + Y_{C.A.L_n} + Shunt_n \qquad (3.9)$$

The other admittances are the mutual admittances of the nodes, and each equals the negative of the sum of all admittances connected directly between the nodes identified by the double subscripts.

Relationship between Thevenin's Theorem And Y-Bus Matrix:

According to the theory, in the relation

$$V = Z_{bus} * I \qquad (3.10)$$

the node or bus voltages (V_i, i = 1, ... , n) are the open circuit voltages. Let us assume that the currents injected in buses 1, ... , k - 1 and k + 1, ... , n are zero when a short circuit occurs at bus k . Then Thevenin impedance at bus k is:

$$Z_{th,k} = \frac{V_k}{I_k} = Z_{kk} \qquad (3.11)$$

So to follow the theory, the Z matrix was obtained by inverting the Y matrix and then the diagonal element of the desired bus is our Thevenin impedance(using MATLAB):

$$Z = Y^{-1} \qquad (3.12)$$

$$Z_{th+,7081} = Z_{(7081,7081)} = 0.5628 + j1.8619 \qquad (3.13)$$

3.6   Verifying The Thevenin System

In order to test the Thevenin system, the following tasks were done (using PSSE):

First the 96 bus system was tested by making the Wind-turbine generator produce 9MW

of power. Then by Power Flow analysis, the voltage at bus 7081 was recorded.
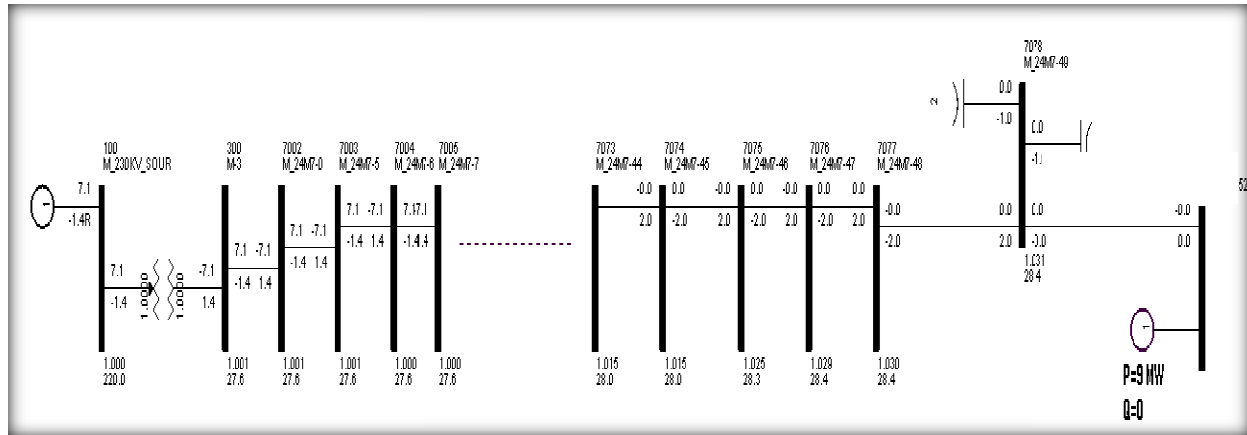
Figure 3.2: Finding the voltage at bus 7081 when Wind-turbine is generating 9MW in 96-bus system

In the next step, the same procedure is performed on the Thevenin system and the

same value for   is expected.
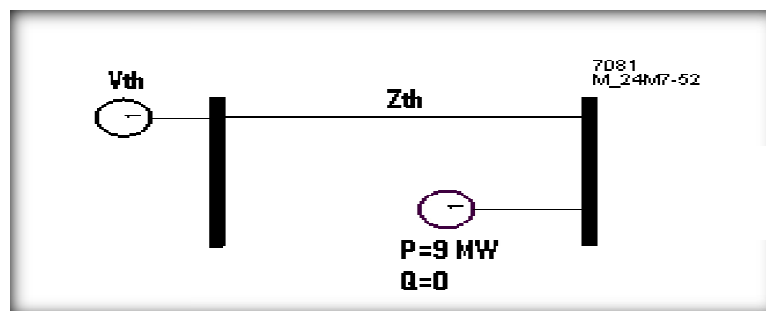
Figure 3.3: finding the voltage at bus 7081 when wind-Turbine is generating 9MW in Thevenin system

The result of the above test verified that the Thevenin system is accurate and has the

same characteristics of the 96-bus system.

$$V_{7081_{96\,bus\,system}} = V_{7081_{Thevenin\,system}} = 1.06\ Perunit \qquad (3.14)$$

3.7 Optimization Algorithm

After creating the two bus system, some boundaries and assumptions had to be considered in order to optimize the result:

Boundaries:

$$P_{Wind-min} \leq \boldsymbol{P_{Wind}} \leq P_{Wind-max} \qquad (3.15)$$

$$\boldsymbol{Q_{Wind}} = 0\ (unity\ power\ factor) \qquad (3.16)$$

$$S_{flywheel-min} \leq \boldsymbol{S_{flywheel}} \leq S_{flywheel-max} \qquad (3.17)$$

$$P_{flywheel-min} \leq \boldsymbol{P_{flywheel}} \leq P_{flywheel-max} \qquad (3.18)$$

$$Q_{flywheel-min} \leq \boldsymbol{Q_{flywheel}} \leq Q_{flywheel-max} \qquad (3.19)$$

$$V_{PCC-min} \leq \boldsymbol{V_{PCC}} \leq V_{PCC-max} \qquad (3.20)$$

$$\delta_{PCC-min} \leq \boldsymbol{\delta_{PCC}} \leq \delta_{PCC-max} \qquad (3.21)$$

Assumptions:

1. P_{wind} changes from 0 to 0.09 Per-unit with 0.01 steps =>

$$P_{wind} = 0\ ,0.01\ ,0.02\ ,0.03\ ,\ldots,0.08\ ,0.09 \qquad (3.22)$$

$S_{flywheel}$ is limited between 0 and 1 (Per-unit)

$$0 \leq S_{flywheel} \leq 1 \qquad (3.23)$$

2. $P_{flywheel}$ is limited between -1 and 1 (Per-unit)

$$-1 \leq P_{flywheel} \leq 1 \qquad (3.24)$$

3. $Q_{flywheel}$ is limited between -2 and 2 (Per-unit)

$$-2 \leq Q_{flywheel} \leq 2 \tag{3.25}$$

4. Voltage at PCC is limited between 0.99 and 1.01 (Per-unit)

$$0.99 * Vth \leq V_{PCC} \leq Vth * 1.01 \tag{3.26}$$

5. Angle at PCC is limited between –Pi and Pi =>

$$-\pi \leq \delta \leq \pi \tag{3.27}$$

Other necessary steps in doing optimization are:

-   Setting of the constraints

-   Setting of the objective function of the system.

Considering the 2 bus model, equations were derived that relate the following elements of the system together (Fig. 3.4):

$$P_{wind}, P_{flywheel}, Q_{flywheel}, V_{PCC}, \delta_{PCC}, V_{thev} \text{ and } Z_{thev}$$
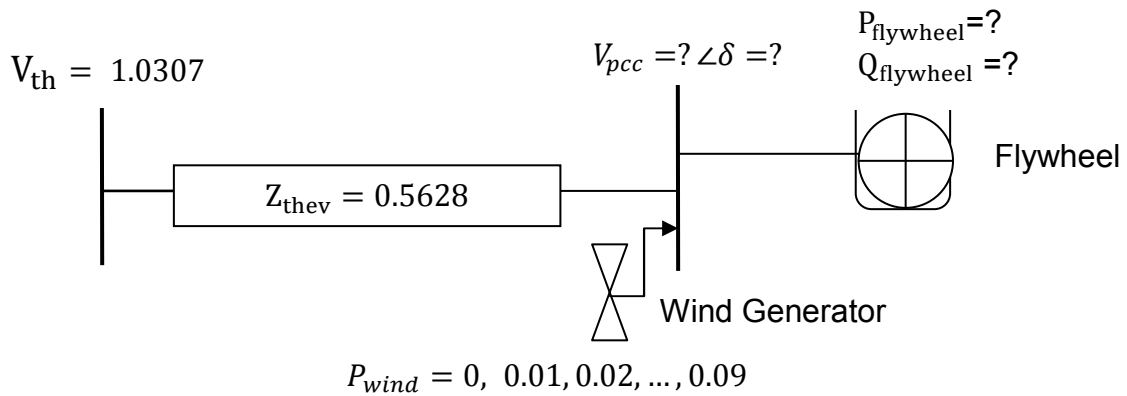
Fig. 3.4 Representation of the Equivalent System

Then the objective function has to be assigned, which in this case is finding the minimum value of the Apparent Power S of the Flywheel in order to keep the $V_{PCC} = 1$

Consider the base MVA values of:

$$S_{Base} = 100.0 \ (MVA) \tag{3.28}$$

$$V_{ll-Base} = 27.6 \ (kV) \tag{3.29}$$

$$Z_{Base} = \frac{V_{ll-base}^2}{S_{base}} \tag{3.30}$$

$$Z_{actual} = Z_{per-unit} \times Z_{Base} \tag{3.31}$$

$$a = \frac{1}{V_{thev}} \tag{3.32}$$

$$P_{wind} = [0, 0.01 \ , 0.02 \ , 0.03 \ , 0.04 \ , 0.05 \ , 0.06 \ , 0.07 \ , 0.08 \ , 0.09] \ \text{(Per-unit)} \tag{3.33}$$

The challenge is to determine optimal values for:

$$P_{flywheel} = ? \quad Q_{flywheel} = ? \quad V_{pcc} = ? \quad \delta_{pcc} = ?$$

Consider the power flowing into the PCC bus from the thevenin's equivalent as below:

$$\left[\frac{\frac{1}{a} - V_{pcc} \angle \delta}{Z_{thev-P.U.}} \right]^* . V_{pcc} \angle \delta = -P_{wind} + P_{flywheel} + jQ_{flywheel} \tag{3.34}$$

$$\frac{\frac{V_{pcc}}{a} \angle \delta - V_{pcc}^2}{Z_{thev-P.U.}} = (-P_{wind} + P_{flywheel}) + jQ_{flywheel} \tag{3.35}$$

This equation (3.35) is rearranged as below:

$$\frac{V_{pcc}}{a} (Cos\delta + jSin\delta) - V_{2pcc}^2 = (P_{total} + jQ_{flywheel}) * (R_{thev} - jX_{thev}) \tag{3.36}$$

The above equation is divided into 2 separate equations for real and reactive powers and forms the constraints:

Real Elements:
$$\frac{V_{pcc}}{a} Cos\delta - V_{pcc}^2 = P_{total}R_{thev} + Q_{flywheel}X_{thev} \tag{3.37}$$

Imaginary Elements:
$$\frac{V_{pcc}}{a} Sin\delta = Q_{flywheel}R_{thev} - P_{total}X_{thev} \tag{3.38}$$

Third equation is:
$$S_{flywheel} = \sqrt{P_{flywheel}^2 + Q_{flywheel}^2} \tag{3.39}$$

Objective Function:

The objective function is chosen to minimize the inverter size. The best way is minimizing the apparent power of the flywheel which will reduce the current through the inverters and consequently reducing the size of the inverter. Minimizing the apparent power is also a cheaper solution. Thus the objective is:

$$\text{Minimum } S_{flywheel} = \sqrt{P_{flywheel}^2 + Q_{flywheel}^2} \tag{3.40}$$

3.8 Complete Formulation

In conclusion, the objective of the problem is defined by (3.40) and it is subject to equality constraints (3.37) – (3.39) and inequality constraints (3.15) to (3.21). This is solved using 'fmincon' function in Matlab.

Chapter 4

TESTS and RESULTS

4.1 Outcome from the Algorithm

The complete formulation was solved for the formulation with objective (3.40) and constraints (3.37) – (3.39) and (3.15) to (3.21). The following results (Table 4.1) were achieved after running the optimization algorithm for positive sequence (Using MATLAB):

Pw	$P_{flywheel}+$	$Q_{flywheel}+$
0	-3.15E-08	-3.43E-07
0.01	-1.69E-09	-9.61E-09
0.02	2.64E-08	-1.26E-07
0.03	0.000576	-0.002342921
0.04	0.001045	-0.00459828
0.05	0.001397	-0.006700473
0.06	0.00164	-0.008643174
0.07	0.001782	-0.010421475
0.08	0.001832	-0.012029588
0.09	0.001798	-0.013463244

Table 4.1: Results of P and Q of the flywheel in order to keep Vpcc within the limit
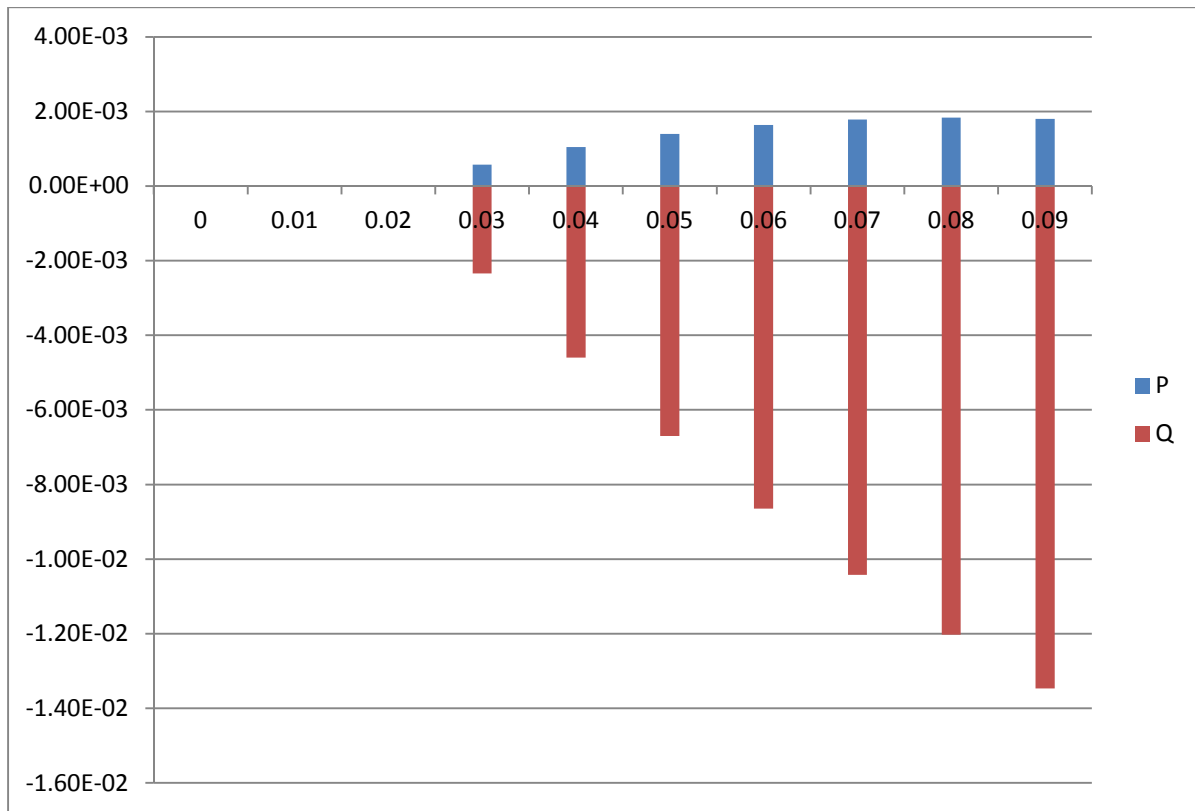
Figure 4.1: Ratios of P and Q of the flywheel with respect to Pwind

Due to the fact that the system is unbalanced, all the steps above have to be repeated for zero sequence as well. The final results are in Table 4.2.

The data in Figure 4.2 demonstrates the values of P and Q that have to be used as a reference in order to keep the Voltage at PCC within the 1% limit.

	(V$_+$=1.0307) (V$_0$=1.1199) (LOAD AT 100%)				
Pw	P+	Q+	P0	Q0	ST
0	-3.15E-08	-3.43E-07	3.95E-07	4.86E-07	1.20E-06
0.01	-1.69E-09	-9.61E-09	0.000757352	-0.001712873	0.001872853
0.02	2.64E-08	-1.26E-07	0.002107598	-0.005332927	0.005734546
0.03	0.000576	-0.002342921	0.003031538	-0.008704941	0.014043273
0.04	0.001045	-0.00459828	0.003550202	-0.011782775	0.021737075
0.05	0.001397	-0.006700473	0.003693278	-0.014520254	0.028671771
0.06	0.00164	-0.008643174	0.003499366	-0.016872259	0.034826174
0.07	0.001782	-0.010421475	0.003016445	-0.018799668	0.04018567
0.08	0.001832	-0.012029588	0.002300295	-0.020266432	0.044733039
0.09	0.001798	-0.013463244	0.00141396	-0.02124597	0.048458392

Table 4.2: Power sequences of the flywheel in order to keep Vpcc within the limit

4.2 Test Results

After the algorithm was simulated successfully, next step was the actual implementation of it into the controller drives. The goal was achieved by using SYPT Pro software and the concept of look-up tables. Test result was successful, because according to look-up tables the drives were choosing the right amount of active and reactive power as a reference point to deliver.

37

4.3 Implementation of the Algorithm In The Control Drive As Look-Up Tables

In order to upload the optimization algorithm into the flywheel system, it was necessary to communicate with controller Drives.

The best possible way to communicate to control system was to use look-up tables. Therefore 20 tables got implemented and each table had all the data from figure 6 for cases of different Load percentage and shunt capacitors situation (ON/OFF) [19]. Also inside the program a function was implemented that uses linear interpolation for special cases. For example if:

$$0.01 < P_{wind-Turbine} = 0.015 < 0.02 \tag{4.1}$$

Then the program calculates the appropriate values of $P_{flywheel}$ and $Q_{flywheel}$ using interpolation:

If the two known points are given by the coordinates (x0,y0) and (x1,y1), the linear interpolant is the straight line between these points. For a value x in the interval (x0,x1), the value y along the straight line is given from the equation:

$$\frac{y - y_0}{x - x_0} = \frac{y_1 - y_0}{x_1 - x_0} \tag{4.2}$$

The final result will be sent into the control system to be used as a reference P and Q.

4.4   Comparison between Different Scenarios

With the intention of understanding the effect of Active Power in voltage regulation, a comparison has been done between the case of $P_{flywheel} = 0$ and $P_{flywheel} \neq 0$. Result shows that when the flywheel injects only reactive Power into the system to regulate the voltage, the value of $S_{flywheel}$ will be slightly higher compare to the time that it injects the combination of P and Q. The following figure shows the difference:
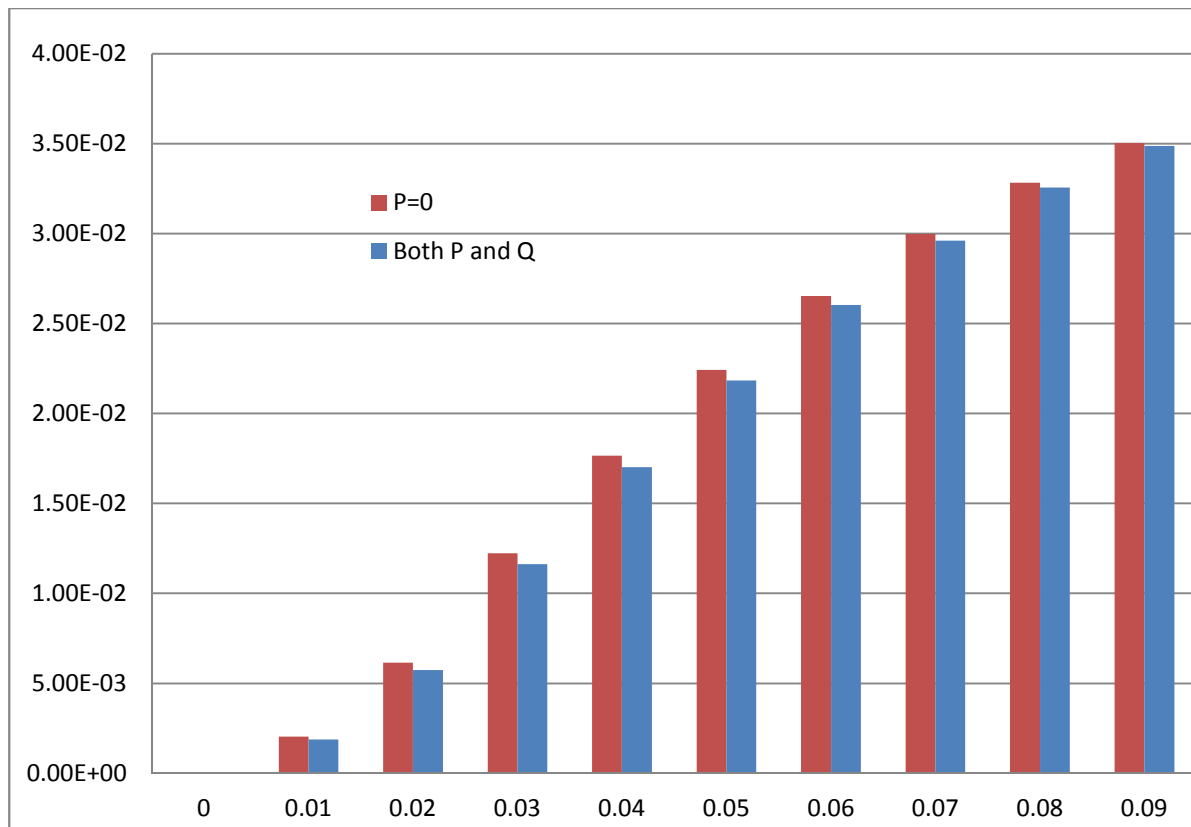
Figure 4.2: comparing the value of Apparent Power when P=0 and P≠0

4.5 Summary

According to this chapter, flywheel is fully capable of voltage regulation and keeping it within the limits. However, the result shows only a small amount of difference between flywheel's performance and the technology that already exists.

Chapter 5

CONCLUSION AND FUTURE WORK

5.1 Conclusion

The thesis proposes a new control scheme for flywheel in conjunction with feeder models to optimally control voltage at point of common coupling. The modeling and analysis of a flywheel energy storage system for voltage regulation has been presented. A control system has been proposed for voltage regulation and energy control.

In conclusion, proprietary control techniques built on customer specifications that give Temporal Power a superior product that has been validated. The outcomes of this project's development work are:

a) A PC based control system for Temporal Power's flywheel system. This control system with the flywheel is readily deployable for a demo. The control system would have hardware and software components.

b) A theoretical model of the flywheel, drive system and control system that would enable potential customers of this flywheel to simulate the flywheel. Through simulation, potential customers would be enabled to ascertain benefits of the flywheel for their system.

c) A tuning method for the control system so that it fits potential customer requirements.

REFERENCES

[1]   G. Genta, *Kinetic Energy Storage*, University Press, Cambridge, 1985.

[2]   A. Ter-Gazarian, *Energy Storage Systems For Power Systems*, IEE Power and Energy Series, 1994.

[3]   J. G. Ciezki, R. W. Ashton, "Selection and stability issues associated with a Navy shipboard DC Zonal electric distribution system," *IEEE Transactions on Power Delivery*, Vol. 15, No. 2, pp. 665-669, April 2000.

[4]   Math. H. J. Bollen, *Understanding Power Quality Problems*, IEEE Press, 2000.

[5]   A. T. Adediran, H. Xiao and K.L. Butler, "Fault Studies of an U.S. Naval Shipboard Power System," NAPS, Univerity of Waterloo, Canada, pp 1-18 to 1-25, October 2000.

[6]   R. S. Weissbach, G. G. Karady and R. G. Farmer, "Dynamic Voltage Compensation on Distribution Feeders using Flywheel Energy Storage," *IEEE Transactions on Power Delivery*, Vol.14, No.2, pp. 465-471, April 1999.

[7]   *PSCAD/EMTDC User's Manual*, Manitoba HVDC Research Center, Manitoba, Canada.

[8]   B. K. Bose, *Modern Power Electronics and AC Drives*, Prentice Hall PTR, 2002.

[9]   *Field Oriented Control of 3 phase AC Motors*, BPRA073, Texas Instruments Europe, 1998.

[10]   D. W. Novotny and T. A. Lipo, *Vector Control and Dynamics of AC Drives*, Oxford Science Publications, 1997.

[11]   P. L. Jansen and R. D. Lorenz, "A Physically Insightful Approach to the Design and Accuracy Assessment of Flux Observers for Field Oriented Induction Machine

Drives," *IEEE Transactions on Industry Applications,* Vol 30, No. 1, pp. 101-110, Jan/ Feb., 1994.

[12] W. Dib, A. Barabanov, R. Ortega, and F. Lamnabhi-Lagarrigue, "An explicit solution of the power balance equations of structure preserving power system models," *IEEE Trans. Power Syst.*, vol. 24, no. 2, pp. 759–765, May 2009.

[13] Keyou Wang, Mariesa L. Crow, "Power System Voltage Regulation via STATCOM Internal Nonlinear Control," IEEE TRANSACTIONS ON POWER SYSTEMS, VOL. 26, NO. 3, pp.1252-1262, August 2011.

[14] M. Subkhan, M. Komori, "New Concept for Flywheel Energy Storage System Using SMB and PMB," *IEEE Transactions On Applied Superconductivity, Vol. 21, No. 3,* June 2011

[15] Trong Duy Nguyen, King Jet Tseng, Shao Zhang, Hoan Thong Nguyen, "On The Modeling and Control of a Novel Flywheel Energy Storage System," *IEEE Conference on Industrial Electronics (ISIE),* pp. 1395 – 1401, 2010

[16] Zhang Yaou, Zhao Wansheng, and Kang Xiaoming, "Control of the Permanent Magnet Synchronous Motor Using Model Reference Dynamic Inversion," *Wseas Trans. On Systems and Control, Issue 5, Vol. 5, pp. 301 – 311*, May 2010.

[17] Oliveira, J.G. "Power electronics and control of two-voltage-level flywheel based all-electric driveline," *IEEE Conference pp. 1659 – 1665,* June 2011

[18] P.H. Mellor, N. Schofield, D. Howe, "Flywheel and Supercapacitor Peak Power Buffer Technologies", *IEEE Colloquium, Vol 50, pp. 47-52.* 2009

[19] Zhihui Guo, Wenyuan Li, Adriel Lau, Tito Inga-Rojas, and Ke Wang, "Detecting X-Outliers in Load Curve Data in Power Systems", *IEEE Transactions On Power Systems, Vol. 27, No. 2,* 2012

[20] S.M. Drouilhet, "Power Flow Management in a High Penetration Wind-Diesel Hybrid Power System withShort-Term Energy Storage," *presented at Burlington, Vermont, Windpower '99, June 20–23*, 1999

APPENDIX

Creating Y-bus Matrix and calculating $Z_{thevenin}$ in MATLAB

The purpose of this program is to create Y-bus matrix and Calculate Thevenin impedance using Hydro One data.

Load data of Hydro One system

100% Load

Bus Number	Load in Per-Unit	Shunt Caps in Per unit
1	0	0
2	0	0
3	0	0
4	0	0
5	0	0
6	0	0
7	0	0
8	0	0
9	0.003448+0.001435i	0
10	0.003448+0.001435i	0
11	0	0
12	0	0
13	0	0
14	0	0
15	0	0
16	0	0
17	0	0
18	0	0
19	0	0
20	0	0
21	0.006003+0.019088i	0
22	0	0
23	0	0
24	0	0
25	0	0
26	0	0
27	0	0
28	0.000236+0.000087i	0
29	0.000095+0.000033i	0.003i
30	0	0
31	0	0.003i

32	0	0
33	0.000095+0.000033i	0
34	0.000095+0.000033i	0
35	0	0
36	0.000667+0.000278i	0
37	0.000667+0.000278i	0
38	0	0
39	0	0
40	0	0.003i
41	0	0
42	0	0
43	0	0
44	0	0
45	0	0
46	0	0
47	0	0
48	0	0
49	0.001014+0.000444i	0
50	0.00109+0.000454i	0
51	0	0
52	0	0
53	0	0
54	0	0
55	0	0
56	0	0
57	0	0
58	0	0
59	0	0
60	0	0
61	0	0
62	0.000318+0.000164i	0
63	0.004368+0.002126i	0
64	0	0
65	0	0
66	0	0
67	0.000236+0.000087i	0
68	0.000212+0.000079i	0
69	0.001886+0.000699i	0
70	0.001886+0.000699i	0
71	0	0
72	0	0
73	0	0
74	0	0
75	0	0
76	0	0
77	0	0
78	0	0

79	0	0.0192i
80	0	0
81	0	0
82	0	0
83	0	0
84	0	0
85	0	0
86	0.0126+0.006102i	0
87	0	0
88	0.001014+0.000444i	0
89	0	0
90	0.0134+0.00649i	0
91	0	0
92	0	0
93	0.002428+0.0009i	0
94	0.002216+0.000821i	0
95	0.000095+0.000033i	0
96	0	0

Branch data of Hydro One system

The following table shows the branch data of Hydro One system used to create Y-bus

Matrix and to calculate Thevenin Impedance.

From Bus	To Bus	R (Perunit)	R0 (Perunit)	X (Perunit)	X0 (Perunit)	b/2 (Perunit)	a
1	2	0.001499	0.001499	0.044975	0.044975	0	1
2	3	0.000804	0.0022	0.00318	0.0086	1.64E-08	1
3	4	0.000402	0.0011	0.00159	0.0043	8.19E-09	1
4	5	0.00067	0.0018	0.00265	0.0072	1.36E-08	1
5	6	0.000268	0.0007	0.00106	0.0029	5.46E-09	1
6	7	0.036859	0.0998	0.145738	0.3952	7.51E-07	1
7	8	0.004289	0.0116	0.016959	0.046	8.74E-08	1
8	9	0.030693	0.0831	0.12136	0.3291	6.25E-07	1
9	10	0.053211	0.1441	0.210393	0.5705	1.08E-06	1
10	11	0.002547	0.0069	0.010069	0.0273	5.19E-08	1
11	12	0.001206	0.0033	0.00477	0.0129	2.46E-08	1
12	13	0.00134	0.0036	0.0053	0.0144	2.73E-08	1
13	14	0.000536	0.0015	0.00212	0.0057	1.09E-08	1
14	15	0.00067	0.0018	0.00265	0.0072	1.36E-08	1

15	16	0.000804	0.0022	0.00318	0.0086	1.64E-08	1
16	17	0.000536	0.0015	0.00212	0.0057	1.09E-08	1
17	18	0.005093	0.0138	0.020138	0.0546	1.04E-07	1
18	19	0.01863	0.0505	0.073664	0.1997	3.79E-07	1
19	20	0.008846	0.024	0.034977	0.0948	1.8E-07	1
20	21	0.000804	0.0022	0.00318	0.0086	1.64E-08	1
21	22	0.000938	0.0025	0.00371	0.0101	1.91E-08	1
22	23	0.003217	0.0087	0.012719	0.0345	6.55E-08	1
23	24	0.005897	0.016	0.023318	0.0632	1.2E-07	1
23	65	0.001206	0.0033	0.00477	0.0129	2.46E-08	1
24	25	0.000804	0.0022	0.00318	0.0086	1.64E-08	1
25	26	0.001206	0.0033	0.00477	0.0129	2.46E-08	1
26	27	0.005629	0.0152	0.022258	0.0604	1.15E-07	1
27	28	0.004557	0.0123	0.018019	0.0489	9.28E-08	1
28	29	0.032972	0.0893	0.130369	0.3535	6.72E-07	1
28	67	0.002547	0.0069	0.010069	0.0273	5.19E-08	1
29	30	0.03019	0.0793	0.074663	0.2124	3.53E-07	1
29	71	0.002547	0.0069	0.010069	0.0273	5.19E-08	1
29	95	0.003619	0.0098	0.014309	0.0388	7.37E-08	1
30	31	0.024196	0.0635	0.05984	0.1703	2.83E-07	1
31	32	0.059165	0.135	0.09813	0.2808	4.1E-07	1
32	33	0.011615	0.0265	0.019265	0.0551	8.04E-08	1
33	34	0.023956	0.0546	0.039734	0.1137	1.66E-07	1
34	35	0.001452	0.0033	0.002408	0.0069	1.01E-08	1
35	36	0.024682	0.0563	0.040938	0.1172	1.71E-07	1
36	37	0.031216	0.0712	0.051774	0.1482	2.16E-07	1
37	38	0.043194	0.0985	0.071641	0.205	2.99E-07	1
38	39	0.030853	0.0704	0.051172	0.1465	2.14E-07	1
39	40	0.0098	0.0224	0.016255	0.0465	6.78E-08	1
40	41	0.013067	0.0298	0.021673	0.062	9.05E-08	1
41	42	0.012341	0.0282	0.020469	0.0586	8.54E-08	1
42	43	0.007985	0.0182	0.013245	0.0379	5.53E-08	1
43	44	0.044646	0.1018	0.074049	0.2119	3.09E-07	1
43	86	0.026134	0.0596	0.043346	0.1241	1.81E-07	1
44	45	0.003267	0.0075	0.005418	0.0155	2.26E-08	1
45	46	0.034483	0.0787	0.057193	0.1637	2.39E-07	1
46	47	0.009074	0.0207	0.015051	0.0431	6.28E-08	1
46	87	0.005808	0.0132	0.009632	0.0276	4.02E-08	1
47	48	0.002178	0.005	0.003612	0.0103	1.51E-08	1
48	49	0.001815	0.0041	0.00301	0.0086	1.26E-08	1
49	50	0.014882	0.0339	0.024683	0.0706	1.03E-07	1
49	88	0.014882	0.0339	0.024683	0.0706	1.03E-07	1
50	51	0.010163	0.0232	0.016857	0.0482	7.04E-08	1
51	52	0.003267	0.0075	0.005418	0.0155	2.26E-08	1
51	89	0.00363	0.0083	0.00602	0.0172	2.51E-08	1
52	53	0.057776	0.1292	0.027111	0.0626	2.45E-06	1
53	54	0.01108	0.0248	0.005199	0.012	4.7E-07	1
54	55	0.01108	0.0248	0.005199	0.012	4.7E-07	1
55	56	0.03799	0.085	0.017826	0.0412	1.61E-06	1
56	57	0.011872	0.0266	0.005571	0.0129	5.03E-07	1
57	58	0.007123	0.0159	0.003342	0.0077	3.02E-07	1

58	59	0.004749	0.0106	0.002228	0.0051	2.01E-07	1
59	60	0.004749	0.0106	0.002228	0.0051	2.01E-07	1
60	61	0.028492	0.0637	0.01337	0.0309	1.21E-06	1
61	62	0.022161	0.0496	0.010399	0.024	9.39E-07	1
62	63	0.078354	0.1753	0.036766	0.0849	3.32E-06	1
63	64	0.022952	0.0513	0.01077	0.0249	9.73E-07	1
65	66	0.002815	0.0076	0.011129	0.0302	5.73E-08	1
67	68	0.015816	0.0428	0.062535	0.1696	3.22E-07	1
68	69	0.004113	0.0083	0.005535	0.0156	2.22E-08	1
68	93	0.017822	0.036	0.023986	0.0677	9.62E-08	1
69	70	0.074029	0.1494	0.099634	0.2812	4E-07	1
71	72	0.007372	0.02	0.029148	0.079	1.5E-07	1
72	73	0.001072	0.0029	0.00424	0.0115	2.18E-08	1
73	74	0.001742	0.0047	0.006889	0.0187	3.55E-08	1
74	75	0.006031	0.0163	0.023848	0.0647	1.23E-07	1
75	76	0.125186	0.339	0.49498	1.3421	2.55E-06	1
76	77	0.051602	0.1397	0.204033	0.5532	1.05E-06	1
77	78	0.016352	0.0443	0.064655	0.1753	3.33E-07	1
78	79	0.007238	0.0196	0.028618	0.0776	1.47E-07	1
79	80	0.011393	0.0309	0.045046	0.1221	2.32E-07	1
80	81	0	0	0.0001	0.0001	0	1
81	82	0	0	0.0001	0.0001	0	1
82	83	0	0	0.0001	0.0001	0	1
83	84	0	0	0.0001	0.0001	0	1
84	85	0	0	0.0001	0.0001	0	1
87	96	0.000233	0.000233	0.0028	0.0028	0	1
89	90	0.005808	0.0132	0.009632	0.0276	4.02E-08	1
90	91	0.011978	0.0273	0.019867	0.0569	8.29E-08	1
91	92	0.014882	0.0339	0.024683	0.0706	1.03E-07	1
93	94	0.094135	0.1899	0.126695	0.3576	5.08E-07	1

Creating Y-bus Matrix and calculating the Thevenin impedance

The following program is written in MATLAB:

```
clear all

clc;

num = 0;          % HONI 96 bus system

percent=100;

Branchdata = Branchdatas(num); % Calling "Branchdatas.m" for Branch Data

Loaddata = Loaddatas(percent);

FromBus = Branchdata(:,1);     % From bus number

ToBus = Branchdata(:,2);     % To bus number

r = Branchdata(:,3);      % Resistance, R

x = Branchdata(:,4);      % Reactance, X

b = Branchdata(:,5);      % Ground Admittance, B/2

a = Branchdata(:,6);      % Tap setting value

BusNum = Loaddata(:,1);   % Bus numbers with loads

yload = Loaddata(:,2);  % Load values in terms of G+jB in P.U.

Shunt = Loaddata(:,3);

z = r + 1i*x;          % Z matrix

y = 1./z;             % To get inverse of each element

b = 1i*b;             % Make B imaginary


nbus = max(max(FromBus),max(ToBus));    % no. of buses
```

```matlab
nbranch = length(FromBus);          % no. of branches

Y = zeros(nbus,nbus);        % Initialise YBus

Zmatrix = zeros(nbus,nbus);


% Formation of the Off Diagonal Elements

for k=1:nbranch

    Y(FromBus(k),ToBus(k)) = Y(FromBus(k),ToBus(k))-y(k)/a(k);

    Y(ToBus(k),FromBus(k)) = Y(FromBus(k),ToBus(k));

end


% Formation of Diagonal Elements

for m =1:nbus

    for n =1:nbranch

        if FromBus(n) == m

            Y(m,m) = Y(m,m) + y(n)/(a(n)^2) + b(n)+ (1*yload(n)) + (Shunt(n));

        elseif ToBus(n) == m && ToBus(n) == nbus

            Y(m,m) = Y(m,m) + y(n) + b(n)+ (1*yload(m)) + (Shunt(m));

        elseif ToBus(n) == m

            Y(m,m) = Y(m,m) + y(n) + b(n);

        end

    end

end


Y                % Bus Admittance Matrix
```

```matlab
X=Y;

X(:,1)=[];

X(1,:)=[];

%Zbus= Y\eye(nbus)     % Bus Impedance Matrix

Zbus=inv(X);

%Zbus=inv(Y)

%H=Zbus*Y;

%Zth80_80=Zbus(80,80)

%Zth3_3=Zbus(3,3)

%Rth=real(Zth);

%Lth=imag(Zth);

Zbus(81,81)
```

Optimization Algorithm

MATLAB was used for optimization. The optimization program includes three parts: Objective function, Constraints and Fmincon function

Fmincon function

```
clear all
clc;
global Rpu Lpu a Rpu0 Lpu0 a0 Pw Smax Smin Qmax Qmin Deltamax Deltamin Pmax Pmin Vmax Vmin Vmax0 Vmin0

%Positive Seq
%  Vth  = 1.0307;        %100
%  Zth  = 0.5628 + 1.8619i; %100
% Vth = 1.0263;          %75
% Zth = 0.539 + 1.8637i; %75
% Vth = 1.0215;          %50
% Zth = 0.5152 + 1.8647i;%50
% Vth = 1.0165;          %25
% Zth = 0.4916 + 1.8650i;%25
Vth = 1.0133;            %10
Zth = 0.4775 + 1.8648i;%10

Rpu=real(Zth);    %Line Resistance
Lpu=imag(Zth);    %Line Inductance
```

```
a=1/Vth;


%  Vth0 = 1.1199;          %100

%  Zth0 = 2.3708 + 4.8472i; %100

% Vth0  = 1.1148;          %75

% Zth0  = 2.1159 + 4.9498i; %75

% Vth0  = 1.106;           %50

% Zth0  = 1.8539 + 5.0238i; %50

% Vth0  = 1.0946;          %25

% Zth0  = 1.5895 + 5.0690i; %25

Vth0    = 1.0866;          %10

Zth0    = 1.4317 + 5.0825i; %10


Rpu0=real(Zth0);     %Line Resistance

Lpu0=imag(Zth0);      %Line Inductance

a0=1/Vth0;




for Pw=0:1:9


Qmin=-3;      Qmax=3;

Smin=0;       Smax=1;

Pmin=-1;      Pmax=1;
```

```
Vmin=Vth-(Vth*0.01);     Vmax=Vth+(Vth*0.01);

Vmin0=Vth0-(Vth0*0.01);    Vmax0=Vth0+(Vth0*0.01);

Deltamin=-2*pi; Deltamax=2*pi;

Stmin=0;           Stmax=1;

options=optimset('algorithm','interior-point','MaxFunEvals',5000,'MaxIter',5000);


lb = [Qmin  Pmin  Vmin  Deltamin  Smin  Qmin  Pmin  Vmin0  Deltamin  Smin  Stmin];
%Defining Lower Boundaries
ub = [Qmax Pmax Vmax Deltamax Smax Qmax Pmax Vmax0 Deltamax Smax Stmax];
%Defining Upper Boundaries


x0 = [0, 0 , 0 , 0 , 0 , 0, 0 , 0 , 0 , 0, 0]; %using initial guesses


[x,fval]=fmincon(@Fun_RV,x0,[],[],[],[],lb,ub,@Confun_RV,options);


ReactivePower=x(1);

ActivePower=x(2);

ApparentPower= x(5);

Pwtemp=Pw+1;

Result(Pwtemp , 1:9) = [ 10, Vth, Vth0, (Pw/100), ActivePower , ReactivePower , x(7),

x(6), x(11)]

end
```

Constraints Function

function [c , ceq] = Confun_RV(x)

global Rpu Lpu a Pw

%Nonlinear inequality Constraints :

c = [];

%Nonlinear equality Constraints :

% [((1/a) - V??) / Z]* . V?? = P + jQ   -> ((V/a)?? - V^2) / Z* = -Pw + P + jQ ->

% (V/a).(Cos? + jSin?) - V^2 = (-Pw + P + jQ) * (R - jX) ->

% (V/a) . Cos(?) - (V^2) = (-Pw+P)R + (-) QX   ->

% (V/a) . Cos(?) - (V^2) - (-Pw+P)R - (+) QX = 0   (1) REAL PART

% (V/a) * Sin(?) = -(+)(-Pw+P)X + QR   ->

% (V/a) * Sin(?) +(-) (-Pw+P)X - QR = 0   (2) IMAGINARY PART

%S = Sqrt(P^2 + Q^2) ->

%S - Sqrt(P^2 + Q^2) = 0   (3) APPARENT POWER

% x(1)-> Q

% x(2)-> P

% x(3)-> V

% x(4)-> Tetha

% x(5)-> S

```
ceq = [( (x(3)/a) * cos(x(4)) ) - ( x(3)^2 ) - ( ((-Pw/100)+x(2)) *Rpu ) + ( x(1)*Lpu ) ; %(1)

    ( (x(3)/a) * sin(x(4)) ) - ( ((-Pw/100)+x(2)) * Lpu ) - ( x(1) * Rpu);  %(2)

    (  x(5) - sqrt ( x(2)^2 + x(1)^2 ) ) %(3)

    ];
end
```

Objective function

```
function f = Fun_RV(x)
```

%Finding the minimum of Apparent Power S = Sqrt(Q^2 + P^2)

```
f = x(5);
```